DNS of transition in hypersonic boundary-layer flows including high-temperature gas effects

By C. Stemmer AND N. N. Mansour

1. Motivation and Objective

Wind-tunnel experiments at hypersonic Mach numbers above 10 are extremely difficult to undertake and facilities are limited. Additionally, the stagnation conditions for free flight under atmospheric conditions can not be reproduced. This results in a limited portability of the wind-tunnel results to atmospheric conditions. Therefore, numerical investigations of hypersonic transition can be extremely valuable in developing an understanding of the transition process at hypersonic speeds.

The objective of this effort is to develop an understanding of effects of nonequilibrium chemistry on transition. Our approach is to compare hypersonic transition on a flat plate under nonequilibrium chemical and thermal conditions to hypersonic transition under equilibrium conditions.

In the 1950's and 60's, a series of hypersonic experiments was conducted in free flight. The transition location could be found but no details on the transitional structures could be recorded in these experiments (see Schneider, 1999, for a comprehensive review of supersonic and hypersonic experiments). Schneider also notes that the angles of attack of the test vehicles are uncertain. An ongoing experiment on transition at $Ma = 21$ in Novosibirsk, Russia Mironov & Maslov 2000, promises experimental verification of the numerical findings to some extent. Further detailed experiments on transition at hypersonic speeds cannot be expected in the near future.

2. Governing Equations

In order not to confuse the index notations, the index i refers to the species 1-5 and no summation is implied on this index, whereas the indices j, k and l refer to the Cartesian directions x, y and z and summation from 1-3 is implied.

The continuity equation for chemically-reacting compressible flows becomes

$$\frac{\partial \rho_i}{\partial t} + \frac{\partial}{\partial x_j}(\rho_i(u_j + u_{i,j}^D)) = W_i, \tag{2.1}$$

where W_i represents the species production terms (see Eq. 2.19) and u_D the diffusion velocities (see Eq. 2.16). Rewriting this equation with the species concentrations rather than the densities, it becomes

$$\rho \frac{Dc_i}{Dt} + \frac{\partial}{\partial x_j}(\rho_i u_{i,j}^D) = W_i, \tag{2.2}$$

where the species concentrations are given by

$$c_i = \frac{\rho_i}{\rho}. \tag{2.3}$$

Note that since

$$\sum_i c_i = 1, \tag{2.4}$$

only $(i-1)$ equations have to be solved.

The total mass is conserved

$$\frac{\partial \rho}{\partial t} + \frac{\partial}{\partial x_j}(\rho u_j) = 0. \tag{2.5}$$

The total momentum equations are

$$\rho \frac{Du_j}{Dt} = -\frac{\partial p}{\partial x_j} + \frac{\partial}{\partial x_k}\tau_{jk} \tag{2.6}$$

with

$$\tau_{jk} = \mu\left(\frac{\partial u_j}{\partial x_k} + \frac{\partial u_k}{\partial x_j}\right) + \delta_{jk}\,\lambda u_{l,l}. \tag{2.7}$$

The bulk viscosity is denoted by λ.

The energy equation for the total energy becomes

$$\rho\,\frac{D(e + u_j u_j/2)}{Dt} = -(q_j + q_j^{vib})_{,j} - (pu_j)_{,j} + \frac{\partial}{\partial x_j}(u_k\,\tau_{jk}) + \sum_i \left((\rho_i h_i u_{i,j}^D)_{,j}\right) \tag{2.8}$$

where e describes the internal energy.

The energy equation for the vibrational energy e^{vib} in the case of vibrational nonequilibrium is as follows

$$\frac{\partial e^{vib}}{\partial t} + \frac{\partial}{\partial x_j}\left(e^{vib}(u_j + u_j^D)\right) = -q_j^{vib} + Q^{T-V} + Q^{chem}. \tag{2.9}$$

For the equilibrium case, the vibrational temperature T^{vib} is equal to the translational temperature T and eq. (2.33) is used with T replacing T^{vib}.

The internal energy for the complete system is a sum of the species internal energies taking into account their concentrations,

$$e = \sum_i c_i e_i. \tag{2.10}$$

The equilibrium internal energy for one species consists of the translational, rotational and vibrational energy and the heat of formation. Note that atoms (N and O) deliver no vibrational and rotational contribution to the internal energy

$$e_i = e_i^{trans}(T) + e_i^{rot}(T) + e_i^{vib}(T^{vib}) + \Delta h_i^f. \tag{2.11}$$

The internal energy contributions from translation, rotation and vibration are assembled through the specific heats at constant volume as

$$e_i = c_{v,i}^{trans} T + c_{v,i}^{rot} T + c_{v,i}^{vib} T^{vib} + \Delta h_i^f. \tag{2.12}$$

The enthalpy is expressed as

$$h_i = c_{p,i}^{trans} T + c_{p,i}^{rot} T + c_{p,i}^{vib} + \Delta h_i^f. \tag{2.13}$$

The internal energy and enthalpy are connected through

$$h = e + \frac{p}{\rho}. \tag{2.14}$$

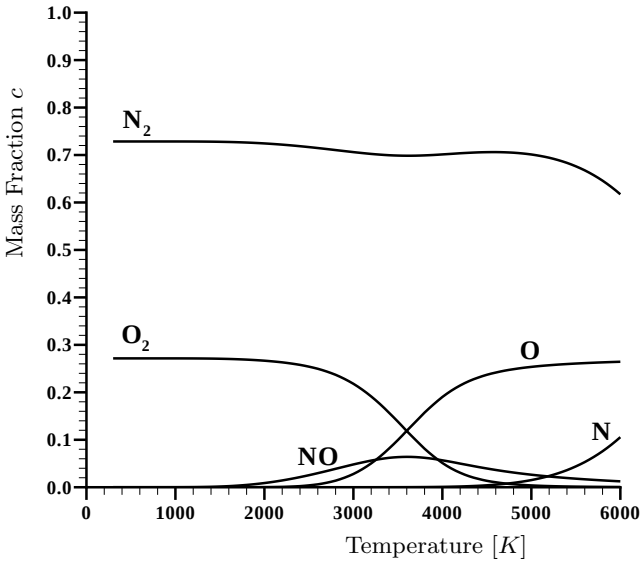

FIGURE 1. Composition of equilibrium air at 1 atm.

The fluid is treated as an ideal gas, where the following equation holds

$$p = \sum_i p_i = \sum_i \rho_i \frac{\mathcal{R}}{M_i} T. \tag{2.15}$$

For the diffusion velocities u_D, Fick's law of diffusion is employed

$$\rho_i u_j^D = -\rho D \frac{\partial c_i}{\partial x_j}, \tag{2.16}$$

where the diffusion coefficient is independent of the species.

The translational and the vibrational heat conduction is described through Fourier's law

$$q_j = -\kappa \frac{\partial T}{\partial x_j}, \qquad q_j^{vib} = -\kappa^{vib} \frac{\partial T^{vib}}{\partial x_j}. \tag{2.17}$$

2.1. *Chemical Modeling*

A five species (N_2, O_2, N, O, NO) model for air will be applied. The equilibrium composition for air at constant pressure over temperature is shown in Fig. 1. The reaction rates (k_f and k_b) are modeled in an Arrhenius manner according to (Park 1989). The model proposed by Park takes into account the translational as well as the vibrational temperature T^{vib} for each species. The vibrational temperature describes the vibrational relaxation, whereas a translational temperature includes the rotational relaxation, which is assumed to take place instantly. It only takes 9-12 molecule collisions for the rotational relaxation to complete, whereas the vibrational relaxation takes 10^5 molecule collisions to reach a steady state (the same order of magnitude as for the chemical relaxation). The seventeen chemical reactions thought to be sufficient for the modeling of air under the conditions of interest are as follows: (The reaction partner M represents any of the

five species considered; see Park, 1989.)

$$\begin{aligned}
\mathrm{N_2 + M} &\rightleftharpoons \mathrm{N + N + M} && (reac.\ 1)\\
\mathrm{O_2 + M} &\rightleftharpoons \mathrm{O + O + M} && (reac.\ 2)\\
\mathrm{NO + M} &\rightleftharpoons \mathrm{N + O + M} && (reac.\ 3)\\
\mathrm{N_2 + O} &\rightleftharpoons \mathrm{NO + N} && (reac.\ 4)\\
\mathrm{NO + O} &\rightleftharpoons \mathrm{N + O_2} && (reac.\ 5)
\end{aligned} \tag{2.18}$$

with the production terms ($M_{N_2}, M_{O_2}, M_{NO}, M_N and M_O$ represent the species masses) :

$$\begin{aligned}
W_{N_2} &= M_{N_2}(R_1 + R_4)\\
W_{O_2} &= M_{O_2}(R_2 - R_5)\\
W_{NO} &= M_{NO}(R_3 - R_4 + R_5)\\
W_N &= M_N(-2R_1 - R_3 - R_4 - R_5)\\
W_O &= M_O(-2R_2 - R_3 + R_4 + R_5)
\end{aligned} \tag{2.19}$$

where

$$\begin{aligned}
R_1 &= -\sum_i k_{f,1i}\left(\frac{\rho_{N_2}}{M_{N_2}}\right)\left(\frac{\rho_i}{M_i}\right) + \sum_i k_{b,1i}\left(\frac{\rho_N}{M_N}\right)^2\left(\frac{\rho_i}{M_i}\right)\\
R_2 &= -\sum_i k_{f,2i}\left(\frac{\rho_{O_2}}{M_{O_2}}\right)\left(\frac{\rho_i}{M_i}\right) + \sum_i k_{b,2i}\left(\frac{\rho_O}{M_O}\right)^2\left(\frac{\rho_i}{M_i}\right)\\
R_3 &= -\sum_i k_{f,3i}\left(\frac{\rho_{NO}}{M_{NO}}\right)\left(\frac{\rho_i}{M_i}\right) + \sum_i k_{b,3i}\left(\frac{\rho_N}{M_N}\right)\left(\frac{\rho_O}{M_O}\right)\left(\frac{\rho_i}{M_i}\right)\\
R_4 &= -k_{f,4}\left(\frac{\rho_{N_2}}{M_{N_2}}\right)\left(\frac{\rho_O}{M_O}\right) + k_{b,4}\left(\frac{\rho_{NO}}{M_{NO}}\right)\left(\frac{\rho_N}{M_N}\right)\\
R_5 &= -k_{f,5}\left(\frac{\rho_{NO}}{M_{NO}}\right)\left(\frac{\rho_O}{M_O}\right) + k_{b,5}\left(\frac{\rho_{O_2}}{M_{O_2}}\right)\left(\frac{\rho_N}{M_N}\right),
\end{aligned} \tag{2.20}$$

and the forward reaction rates k_f for the five reactions considered are

$$\begin{aligned}
k_{f,1} &= 2.0\times10^{15}\,(\sqrt{TT^{vib}})^{-3/2}\exp(-(59,500/\sqrt{TT^{vib}})) \quad \text{for M = molecule}\\
k_{f,1} &= 1.0\times10^{16}\,(\sqrt{TT^{vib}})^{-3/2}\exp(-(59,500/\sqrt{TT^{vib}})) \quad \text{for M = atom}\\
k_{f,2} &= 7.0\times10^{15}\,(\sqrt{TT^{vib}})^{-8/5}\exp(-(113,200/\sqrt{TT^{vib}})) \quad \text{for M = molecule}\\
k_{f,2} &= 3.0\times10^{16}\,(\sqrt{TT^{vib}})^{-8/5}\exp(-(113,200/\sqrt{TT^{vib}})) \quad \text{for M = atom}\\
k_{f,3} &= 5.0\times10^{9}\exp(-(75,500/\sqrt{TT^{vib}})) \quad \text{for M= } \mathrm{N_2},\ \mathrm{O_2}\\
k_{f,3} &= 1.1\times10^{11}\exp(-(75,500/\sqrt{TT^{vib}})) \quad \text{for M= N, O, NO}\\
k_{f,4} &= 6.4\times10^{11}\,(\sqrt{TT^{vib}})^{-1}\exp(-(38,370/\sqrt{TT^{vib}}))\\
k_{f,5} &= 8.4\times10^{6}\exp(-(19,450/\sqrt{TT^{vib}})).
\end{aligned} \tag{2.21}$$

The backward reaction rates k_b are calculated from the equilibrium rates through

$$k_{b,i} = k_{f,i}/K_{eq,i} \tag{2.22}$$

The equilibrium rates are defined as

$$\begin{aligned}
K_{eq,1} &= \exp(0.50989 \cdot (\sqrt{TT^{vib}}/10,000) + 2.4773 + 1.7132 \cdot \log_{10}(10,000/\sqrt{TT^{vib}}) \\
&\quad -6.5441 \cdot (10,000/\sqrt{TT^{vib}}) + 0.29591 \cdot (10^8/(TT^{vib})) \\
K_{eq,2} &= \exp(1.4766 \cdot (\sqrt{TT^{vib}}/10,000) + 1.6291 + 1.2153 \cdot \log_{10}(10,000/\sqrt{TT^{vib}}) \\
&\quad -11.457 \cdot (10,000/\sqrt{TT^{vib}}) - 0.009444 \cdot ((10^8/(TT^{vib})) \\
K_{eq,3} &= \exp(0.50765 \cdot (\sqrt{TT^{vib}}/10,000) + 0.73575 + 0.48042 \cdot \log_{10}(10,000/\sqrt{TT^{vib}}) \\
&\quad -7.4979 \cdot (10,000/\sqrt{TT^{vib}}) - 0.16247 \cdot ((10^8/(TT^{vib})) \\
K_{eq,4} &= \exp(0.96921 \cdot (\sqrt{TT^{vib}}/10,000) + 0.89329 + 0.73531 \cdot \log_{10}(10,000/\sqrt{TT^{vib}}) \\
&\quad -3.9596 \cdot (10,000/\sqrt{TT^{vib}}) + 0.006818 \cdot ((10^8/(TT^{vib})) \\
K_{eq,5} &= \exp(-0.002428 \cdot (\sqrt{TT^{vib}}/10,000) - 1.7415 - 1.2331 \cdot \log_{10}(10,000/\sqrt{TT^{vib}}) \\
&\quad -0.95365 \cdot (10,000/\sqrt{TT^{vib}}) - 0.04585 \cdot ((10^8/(TT^{vib}))
\end{aligned} \tag{2.23}$$

2.2. *Modeling of physical and transport properties*

The following relations are for a mixture of chemically-reacting gases.

2.2.1. *Specific heat at constant volume*

The specific heat at constant volume c_v for atoms is described through:

$$c_{v,i} = c_{v,i}^{trans} = \frac{3}{2} R_i. \tag{2.24}$$

The partial derivatives of the species concentrations with respect to the temperature are the contributions due to chemical reactions.

The specific heat at constant volume c_v for molecules (Vincenti & Kruger 1982) is made up as follows,

$$\begin{aligned}
c_{v,i} &= c_{v,i}^{trans} + c_{v,i}^{rot} + c_{v,i}^{vib} \\
&= \frac{3}{2} R_i + R_i + \frac{(\Theta_i^{vib}/T^{vib})^2 e^{\Theta_i^{vib}/T^{vib}}}{(e^{\Theta_i^{vib}/T^{vib}} - 1)^2} R_i,
\end{aligned} \tag{2.25}$$

where Θ_i^{vib} is the characteristic temperature of vibration of the molecular species.

2.2.2. *Specific heat at constant pressure*

The specific heat at constant pressure c_p is described by:

$$c_{p,i} = c_{v,i} + R_i T. \tag{2.26}$$

2.2.3. *Viscosity*

Blottner's formula will be employed for the modeling of the viscosity (Blottner, Johnson & Ellis 1971). This approximate formula is valid up to 10,000 K, far exceeding the temperature range of the flows investigated here. The coefficients A_{μ_i}, B_{μ_i} and C_{μ_i} are given by Blottner *et al.*

$$\mu_i = 0.1 \cdot \exp\left[C_{\mu_i} + (\ln T \cdot (B_{\mu_i} + \ln T \cdot A_{\mu_i}))\right]. \tag{2.27}$$

2.2.4. *Thermal conductivity*

The species' thermal conductivities are described employing Eucken's correction, given as (Hirschfelder, Curtiss & Bird 1964):

$$\kappa_i = \mu_i(\frac{5}{2}c_{v,i}^{trans} + c_{v,i}^{rot}), \qquad \kappa_i^{vib} = \mu_i(c_{v,i}^{vib}). \tag{2.28}$$

2.2.5. *Mixing rules for viscosity and thermal conductivity*

The mixing rule in a mixture of gases, according to (Wilke 1950), is

$$\mu_{mix} \approx \sum_{i=1}^{n} \frac{x_i \mu_i}{\sum_{j=1}^{n} x_j \Phi_{ij}} \tag{2.29}$$

with

$$\Phi_{ij} = \frac{\left[1 + (\mu_i/\mu_j)^{1/2}\ (M_j/M_i)^{1/4}\right]^2}{(8 + 8M_i/M_j)^{1/2}}$$

and

$$x_i = \frac{c_i/M_i}{\sum_{j=1}^{n}(c_j/M_j)}.$$

The same formula applies for the thermal conductivities, replacing the viscosity μ by the thermal conductivity k.

Further details of the physical modeling can be found, for example, in (Sarma 2000).

2.2.6. *Diffusion coefficient*

A constant Schmidt number $Sc = 0.5$ is assumed (Hudson 1996) which yields for the diffusion coefficient:

$$D = \frac{\mu}{\rho\, Sc} = \frac{2\,\mu}{\rho} \tag{2.30}$$

2.2.7. *Translational-vibrational energy exchange*

Vibrational energy is present only in the molecular species N_2, O_2 and NO, which are all modeled as harmonic oscillators. Therefore the following equations are valid. In case of the incorporation of anharmonic oscillatory molecules like CO_2, different relaxation and energy expressions have to be applied (Vincenti & Kruger 1982).

The translational-vibrational energy exchange is described through a Landau-Teller relaxation model (Vincenti & Kruger 1982) as,

$$Q^{T-V} = \sum_i c_i \frac{e_i^{vib,eq}(T) - e_i^{vib}(T^{vib})}{\tau_i}, \tag{2.31}$$

where the relaxation times are determined for each species as

$$\tau_i = \frac{1}{p_i} C_1 \exp((C_2/T)^{1/3}), \tag{2.32}$$

and the nonequilibrium vibrational energy depends on the vibrational temperature as

$$e_i^{vib} = \frac{\Theta_i^{vib}/T^{vib}}{e^{\Theta_i^{vib}/T^{vib}} - 1} R_i T^{vib}. \tag{2.33}$$

The equilibrium value for the vibrational energy $e_i^{vib,eq}$ follows the same expression, with T replacing T^{vib}.

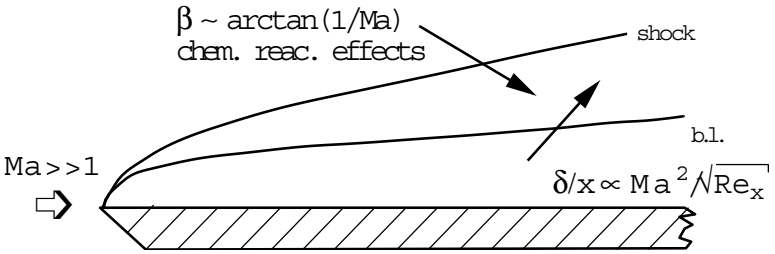

FIGURE 2. Schematic of shock location and boundary-layer edge for hypersonic boundary layers on a flat plate, showing dependence on Mach number

The chemical source term in Eq. 2.9 is expressed as the sum over the vibrational internal energy multiplied with the production terms:

$$Q^{chem} = \sum_i c_i (e_i^{vib} W_i) \tag{2.34}$$

3. Future Work

A spatial finite-difference DNS code will be applied on a Cartesian three-dimensional grid on a flat plate. The code will incorporate a shock-capturing technique, since the shock provoked by the flat-plate leading edge is the major source of nonequilibrium. For the high Mach numbers, the location of the shock and the boundary-layer edge, which is the area of linear instability for hypersonic flows, merge, and the chemical and thermal nonequilibrium in this region is expected to influence transition to a large extent (Fig. 2; see also Anderson, 1989).

For the flight conditions investigated, the data in Fig. 3 are relevant. At a speed of $V_\infty = 5.9$ Km/s, dissociation of nitrogen and oxygen can be expected. For an altitude of $h = 25$ Km, chemical and thermal equilibrium will persist at a Mach number $Ma = 20$. At an altitude of about $h = 100$ Km (Ma=20.8), full nonequilibrium conditions are present. Conditions are chosen such that ionization will not take place. This choice is consistent with the return path of the shuttle as it enters the athmosphere.

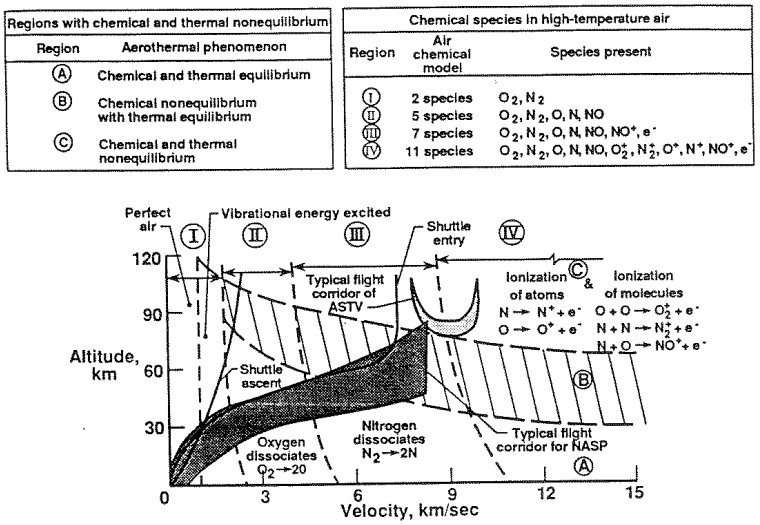

FIGURE 3. Flow regimes and thermochemical phenomena in the stagnation region of a 30.5 cm radius sphere flying in air (Gupta *et al.* 1990)

REFERENCES

ANDERSON, J. D. 1989 *Hypersonic and and High Temperature Gas Dynamics.* AIAA publication.

BLOTTNER, F. G., JOHNSON, M. & ELLIS, M. 1971 Chemically reacting viscous flow program for multi-component gas mixtures. Sandia Natl. Laboratories, SC-RR-70-754.

GUPTA, R. N., YOS, M. J., THOMPSON, R. A. & LEE, K.-P. 1990 *A review of reaction rates and thermodynamic and transport roperties for an 11-species air Model for chemical and thermal nonequilibrium calculations to 30,000K. NASA* RP-1232.

HIRSCHFELDER, J. O., CURTISS, C. F. & BIRD, R. A. 1964 *Molecular Theory of Gases and Liquids.* Wiley & Sons, New York.

HUDSON, M. J. 1996 *Linear Stability of Hypersonic Flows in Thermal and Chemical Nonequilibrium.* Ph.D. Thesis, North Carolina State University, Raleigh, NC.

MIRONOV, S. G. & MASLOV, A. A., Experimental study of secondary stability in a hypersonic shock layer on a flat plate. *J. Fluid Mech.* **412**, 259-277.

PARK, C. 1989 A review of reaction rates in high temperature air. *AIAA* Paper 89-1740.

SARMA, G. S. R. 2000 Physico-chemical modeling in hypersonic flow simulation. *Prog. Aerospace Sci.* **36**, 281-349.

SCHNEIDER, S. P. 1999 Flight data for boundary-layer transition at hypersonic and supersonic speeds. *J. Spacecraft and Rockets* **36**, 8-20.

VINCENTI, W. G. & KRUGER. C. H. 1982 *Introduction to Physical Gas Dynamics.* Krieger, Malabar, FL.

WILKE, S. P. 1950 A Viscosity Equation for Gas Mixtures. *J. Comp. Phys.* **18**, 517-519.